Instrumented Impact Testing of Ceramics

Transactions of the Japan Institute of Metals, Vol. 27, No. 10 (1986), pp. 775 to 783

Instrumented Impact Testing of Ceramics*

By Toshiro Kobayashi**, Mitsuo Niinomi**, Yoshihiro Koide*** and Kenji Matsunuma****

Many researches on ceramics have been reported, but brittleness is a key problem to be overcome. However, no generalized method on impact test of ceramics has been reported.

The total absorbed energy evaluated from the Charpy impact test for brittle materials includes largely the energy absorbed by the machine and the kinetic one of the broken specimen, in addition to the real fracture one of the specimen. These energies, therefore, must be exactly analyzed and then the real fracture one is to be evaluated.

In this study, the absorbed energy of partially stabilized zirconia (PSZ) and SiC is analyzed in the instrumented Charpy impact test and in the static three-point bend test. Moreover, the influence of stress-induced phase transformation on the toughness in PSZ is investigated.

As a result, it is shown that the real fracture energy of PSZ is 57–59% of the total absorbed one and that the one of SiC is 38–56%. It is also shown that the amount of stress-induced phase transformation in the impact test is more than the one in the static three-point bend test. Furthermore, it is pointed out that a singularly oscillated loading is found in the impact test of PSZ, which is due probably to the co-working effect between the inertia effect and the stress-induced phase transformation during the dynamic fracture.

(Received April 28, 1986)

Keywords: *instrumented impact test, ceramics, stress-induced transformation, partially stabilized zirconia, silicon carbide, brittle material, dynamic fracture*

I. Introduction

Recently, much attention has been paid to ceramics as new engineering materials. It can be said that the reliability of new ceramics has been much more improved compared with the old ceramics. This improvement has been achieved by detailed investigations on properties, for example, thermal resistance and mechanical properties and by applying these results to material design based on purified raw materials.

However, from the view of structural application, it is the most important problem to overcome the brittleness. However, the toughness test, especially the impact toughness test on brittle materials like ceramics has been hardly carried out and in fact no generalized method has been reported. Hitherto, it is suggested that the most important problem is the difficulty for the evaluation of the real energy of specimen itself, because the excess energy other than the real fracture one of specimen is fairly included in the impact one of brittle materials like ceramics[1]. For this restriction, a unique method has been reported. According to this method, the specimen itself is swung down against the anvil stopper from the angle at which the fracture has just occurred; the impact energy is determined from this critical lifting angle[2]. The excess energy is not included in this method. However, this is very complicated and contains the possibility of change in material properties by repeated impact.

In this study, a new small type instrumented Charpy impact test machine has been developed to effectively evaluate the dynamic toughness of ceramics. Load-deflection curves and the absorbed energy are analyzed using

---

* This paper was originally published in Japanese in J. Japan Inst. Metals, **50** (1986), 299.

** Department of Production Systems Engineering, Toyohashi University of Technology, 1-1, Hibarigaoka, Tempaku-cho, Toyohashi, Aichi, 440, Japan.

*** Graduate Student, Toyohashi University of Technology. Present address: Nippon Kokan K. K.

**** Graduate Student, Toyohashi University of Technology.

this machine, and the analyzing method of impact properties of brittle materials is investigated in detail. Moreover, the influence of stress-induced tetragonal-to-monoclinic phase transformation on the dynamic fracture in partially stabilized zirconia (PSZ) is investigated.

II. Experimental Procedure

1. Specimen

Partially stabilized zirconia (PSZ: ZrO_2–3 mol%Y_2O_3) and SiC were used in this study. Both specimens were ground after sintering by hot-pressing. Geometries of test specimens are shown in Fig. 1. The specimen (b) is based on JIS R-1601-1981.

2. Instrumented Charpy impact test and static three-point bend test

The specimens (a) and (b) were tested by a 14.7 J instrumented Charpy impact testing machine at room temperature. This machine was newly developed for the present study. Strain gauges were attached near the tup of the hammer, and a film potentiometer was set up at the rotating axis of the hammer. Load-deflection signals were detected by these sensors and directly transferred and analyzed by a computer system. Essentials of this method have been reported elsewhere[3]. Impact velocities were 1.5 m/s (energy capacity: 1.8 J) for PSZ (a$\cdots$ this shows specimen type of Fig. 1), 0.95 m/s (0.72 J) for PSZ(b), 0.76 m/s (0.46 J) for SiC(a) and 0.12 m/s (0.38 J) for SiC(b). Shapes of load-deflection curves were ascertained not to be influenced by these different conditions[4]. The static three-point bend test on the specimen (b) of PSZ and SiC was carried out at room temperature according to JIS R-1601-1981. Also in this case, deflection and load signals were detected to measure the absorbed energy. The load-deflection curves were recorded by an X–Y recorder.

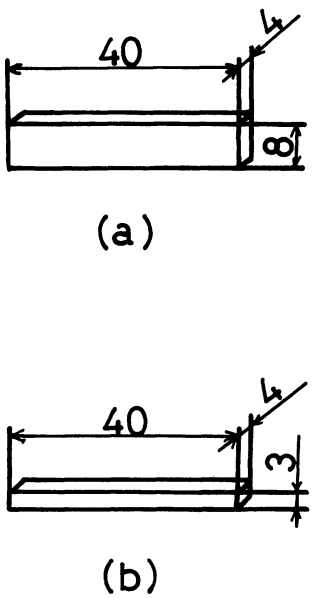

Fig. 1 Geometry of test specimens.

3. X-ray diffraction analysis of PSZ

The influence of stress-induced tetragonal-to-monoclinic phase transformation in PSZ was investigated by X-ray diffraction with Geiger flex 2028 made by Rigaku Denki on the fracture surfaces after the Charpy impact test and the static three-point bend test and on the sintered surface before grinding. The target and filter were Co and Fe, respectively.

III. Results and Discussion

1. Instrumented impact test and static three-point bend test

Typical load-deflection curves are shown in Fig. 2. Each curve shows linear loading up to the maximum load except PSZ(a), although a little inertia load effect exists. Therefore, it is said that macroscopic plastic deformation does not exist, hence the curve falls vertically from the maximum load to zero load level. Generally, the absorbed energy (E_t) evaluated from the total area under the load-deflection curve is represented by

$$E_t = E_i + E_p, \tag{1}$$

where E_i is the apparent crack initiation energy absorbed up to the maximum load and E_p is the apparent crack propagation one absorbed after the maximum load. $E_t \simeq E_i$ is obtained analyzing the load-deflection curves in this study; i.e., the materials used in this study showed an elastic type brittle fracture.

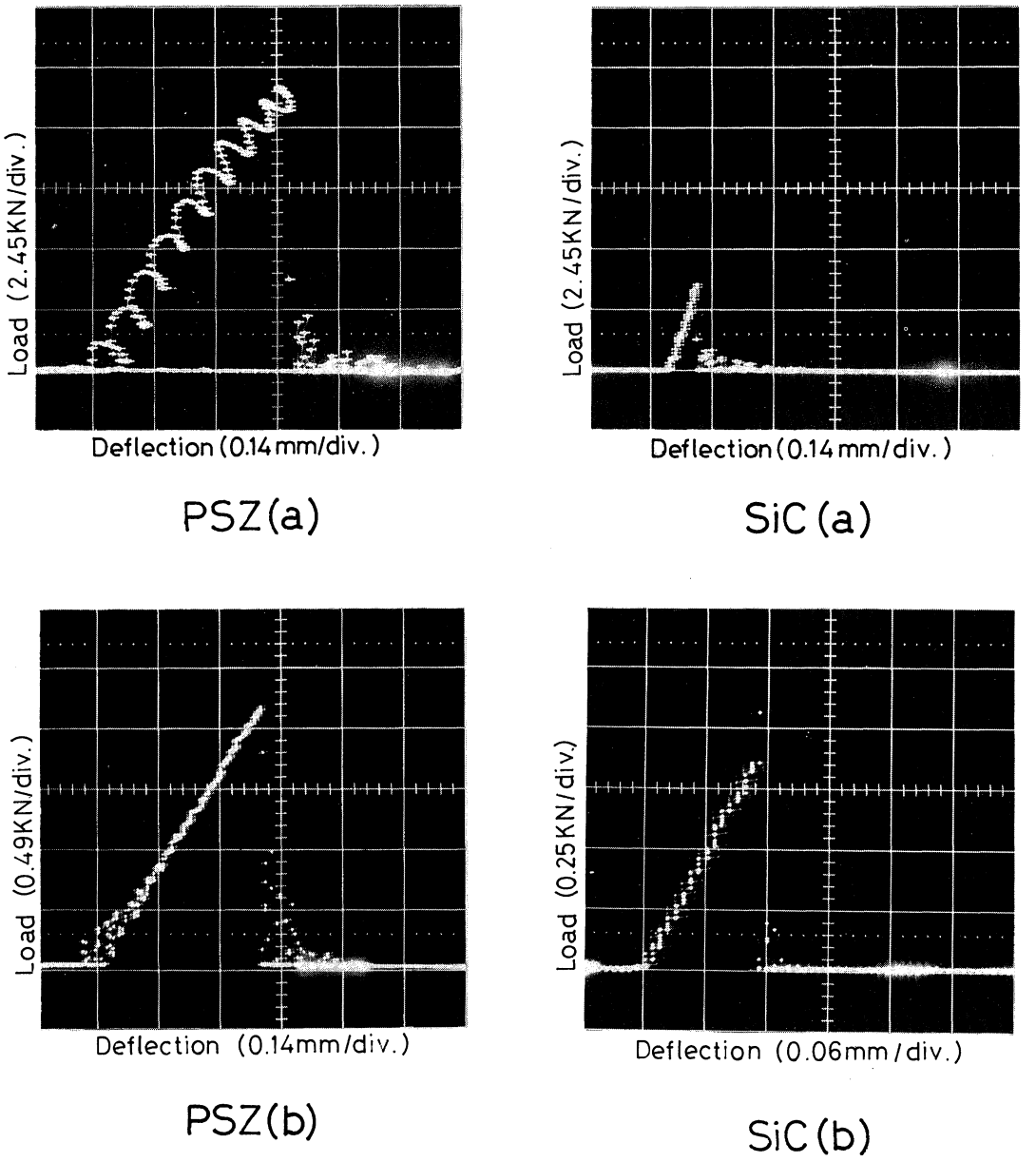

Fig. 2 Typical load-deflection curves of each specimen.

The load-deflection curve of PSZ(a) shows a singular spiral-like loading up to the maximum load. This interesting phenomenon has been found first in the present study.

2. Analysis of absorbed energy in instrumented impact test

Generally, the total absorbed energy E_t (in the present study, the value by dial reading was used) obtained from impact test contains the excess energy E_m, which is mainly spent for elastic deformation of testing machine, and the kinetic energy E_k, which is spent to toss the broken specimen, in addition to the real fracture energy E_f which is required to deform and break the specimen itself. It is necessary, therefore, to remove these excess energies from E_t, in order to evaluate the real fracture energy

of specimen, E_f.

The total absorbed energy E_t may be analyzed and described as follows.

$$E_t = E_s + E_m = E_f + E_k + E_m. \quad (2)$$

E_t is composed of E_m, which is spent for the elastic deformation of testing machine, and E_s which is absorbed and stored in the specimen. Moreover, E_s is divided into E_f and E_k.

The total compliance C_t, which is measured as the reciprocal of initial slope of the load-deflection curve, consists of the machine compliance (C_m) and the specimen compliance (C_s). Therefore, C_t is given by the following equation[3].

$$C_t = C_s + C_m. \quad (3)$$

C_s is non-linear beyond the elastic limit, and therefore, required to be corrected in the plastic region. However, this correction is not necessary in this case, as all the specimens used in this study showed an elastic type brittle fracture. The compliance of unnotched specimens is theoretically given by the equation[5],

$$C_s = (l^3/4W^3EB)\cdot(1+2.85(W/l)^2 - 0.84(W/l)^3), \quad (4)$$

where E is Young's modulus, l is the length between the supports, B is the specimen thickness and W is the specimen width. C_m was indirectly defined by measuring C_t on the load-deflection curve, which was obtained from the instrumented Charpy impact test, and by substituting C_s theoretically calculated by eq. (4) for eq. (3). Each evaluated compliance is shown in Table 1.

As mentioned before, the specimens in the present study were fractured in the elastic loading region. Therefore, E_m is approximately given by using the machine compliance as follows[3].

$$E_m = E_t(C_m/C_t). \quad (5)$$

The theoretical calculation of kinetic energy E_k is attempted in the following manner. The hammer velocity of Charpy impact test machine just before impacting is V_0; then, the specimen bends and finally a crack initiates and propagates. It is considered that the energy which is spent to reduce the hammer velocity from V_0 to V_f (final hammer velocity at fracture) is equivalent to that which is spent for the elastic deformation and crack surface formation in the specimen and the elastic deformation of machine. As the elastic energy stored in the specimen and the machine is released at fracture, the specimen is generally tossed forward. Although it is considered actually that a part of E_m is added to the real kinetic energy of the broken specimen halves, E_k defined by eq. (2) assumes that only a part of the elastic energy stored in the specimen (E_s) is spent as the kinetic one. Therefore, it is assumed that the specimen is tossed from the hammer of the velocity of V_f and E_k is estimated. Assuming that the relation between hammer and fractured specimen is replaced by the problem of collision with a linear motion, E_k is approximated by the following equation on the basis of the law of the conservation of momentum.

Table 1 Total, specimen, and machine compliances (respectively C_t, C_s and C_m).

Specimen	C_t ($\times 10^{-4}$ mm/N)	C_s ($\times 10^{-4}$ mm/N)	C_m ($\times 10^{-4}$ mm/N)
PSZ(a)	0.357	0.210	0.147
SiC(a)	0.209	0.083	0.126
PSZ(b)	3.290	1.980	1.310
SiC(b)	1.390	0.784	0.606

Table 2 Analysis of absorbed energy by 14.7 J instrumented Charpy impact testing machine.

Specimen	e	E_t (J)	E_m (J)	E_s (J)	E_k (J)	E_f (J)	E_f/E_t (%)
PSZ(a)	0.30	1.56	6.45×10^{-1}	9.15×10^{-1}	1.75×10^{-3}	9.13×10^{-1}	59.5
SiC(a)	0.39	9.77×10^{-2}	5.88×10^{-2}	3.89×10^{-2}	1.70×10^{-3}	3.72×10^{-2}	38.1
PSZ(b)	0.30	3.50×10^{-1}	1.39×10^{-1}	2.11×10^{-1}	1.05×10^{-3}	2.01×10^{-1}	57.4
SiC(b)	0.39	1.64×10^{-2}	7.15×10^{-3}	9.25×10^{-3}	1.68×10^{-4}	9.08×10^{-3}	55.5

$$E_k = mM^2/(2(m+M)^2)(1+e)^2V_f^2, \quad (6)$$

where M and m are the masses of hammer and specimen, respectively. e is the coefficient of restitution between hammer and fractured specimen. e was estimated by the following equation[6] applying E_t measured by an indicator, which was obtained from impacting the fractured specimen halves restored by a cellophane tape at various impact velocities.

$$E_t/mV^2 \simeq 1+e. \quad (7)$$

The gradient of $E_t - mV^2$ curve is equal to $1+e$; therefore, e can be obtained. Results of the analysis of absorbed energy for each specimen are shown in Table 2. Evaluated E_f of PSZ is 57–59% of E_t. Evaluated E_f of SiC is 38–56% of E_t. Therefore, it may be assumed that the ratio of the excess energy to E_t becomes larger as the brittleness of material increases.

The absorbed energy in the static three-point bend test was also analyzed by a similar method in the case of instrumented impact test. Consequently, E_f values of PSZ and SiC were evaluated to be 61% and 50% of E_t, respectively. Analyzed results are shown in Figs. 3 and 4.

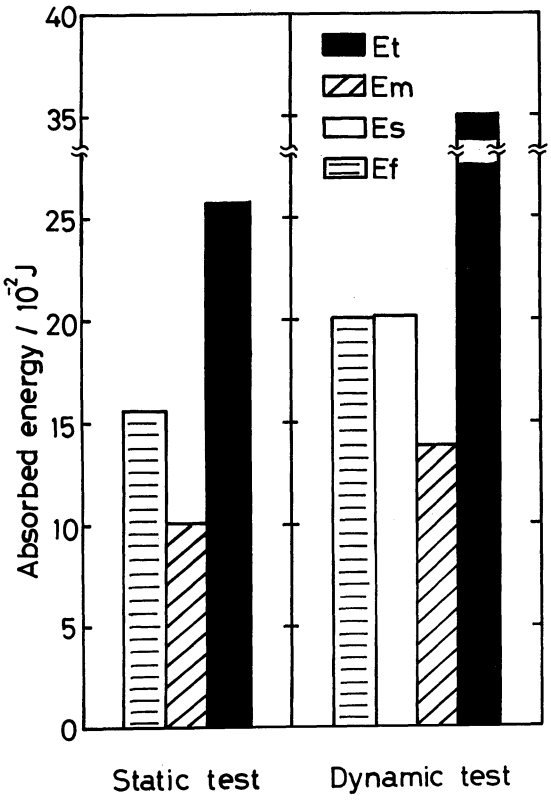

Fig. 3 Analysis of absorbed energy of PSZ(b).

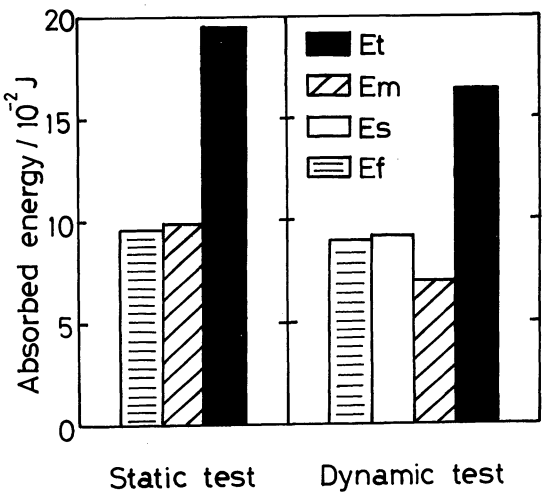

Fig. 4 Analysis of absorbed energy of SiC(b).

3. Comparison of absorbed energy between impact test and static three-point bend test

Although it is generally considered that mechanical properties of brittle materials are slightly dependent on the strain rate, it is expected that the frature energy in the dynamic test is smaller than that in the static test.

The real fracture energy E_f of SiC in the dynamic test was 94% of that in the static three-point bend test. However, E_f of PSZ in the dynamic test is larger than that in the static three-point bend test. It may be considered that this cause is related to the stress-induced phase transformation of PSZ. Further details on this behavior will be discussed later.

4. X-ray diffraction analysis of PSZ

Partially stabilized zirconia contains a metastable tetragonal phase, and this tetragonal phase transforms into the monoclinic phase by stress-induced martensitic transformation in the stress field of crack tip vicinity[7]. It is generally said that a part of energy in the stressed zone is absorbed during the phase transformation and then toughening is expected[8].

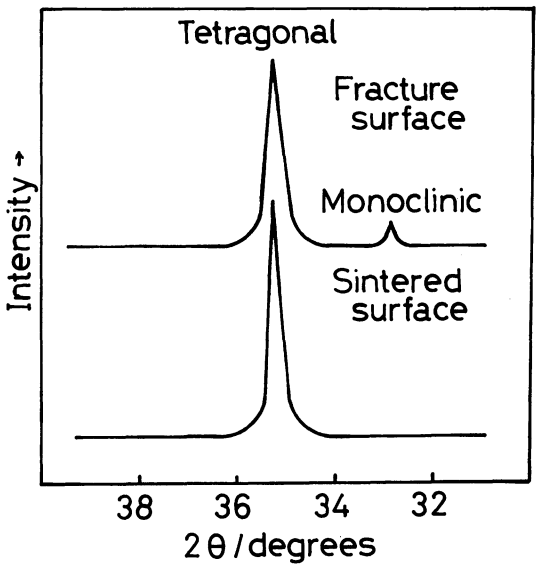

Fig. 5 X-ray diffraction patterns on tetragonal-to-monoclinic phase transformation in dynamic testing of PSZ(a).

Moreover, it has been also reported that the stress-induced phase transformation creates microcracks and these microcracks restrict the macrocrack propagation[9].

X-ray diffraction patterns of as sintered surface and fractured surface of the specimen (a) in the Charpy impact test are shown in Fig. 5. The strong line (111) of the tetragonal phase is observed to originate from the sintered surface. The two strong lines of the tetragonal phase (111) and the monoclinic one ($11\bar{1}$) were observed to originate from the fractured surface in the impact test. From these facts, it has been recognized that the stress-induced tetragonal-to-monoclinic transformation occurs in the impact test.

X-ray diffraction patterns from the fractured surfaces of specimen (b) in the impact test and in the static three-point bend test are shown in Fig. 6. As compared with the results of the measurement of integrated intensity ratio of tetragonal to monoclinic, it is obvious that the amount of stress-induced phase transformation in the impact test is larger than that in the static three-point bend test. Therefore, it is assumed that the stress-induced tetragonal-to-monoclinic phase transformation depends on the strain rate.

However, it is generally known that the deformation-induced transformation in metallic materials appears preferable under the static strain rate condition[10]. This cause is considered to be that the actual temperature of specimen may exceed the M_d point by some adiabatic temperature rise in the case of dynamic deformation[11]. The temperature rise at the crack tip is given by[12]

$$\Delta T = T_c h(\delta) \tag{8}$$

with

$$T_c = 2/3\sqrt{\pi}\cdot(1-\nu^2)\cdot K_{max}^2/E\sqrt{\rho ckt}, \tag{9}$$

where K_{max} is the maximum stress inensity factor, ρ is the density, c is the specific heat, k is

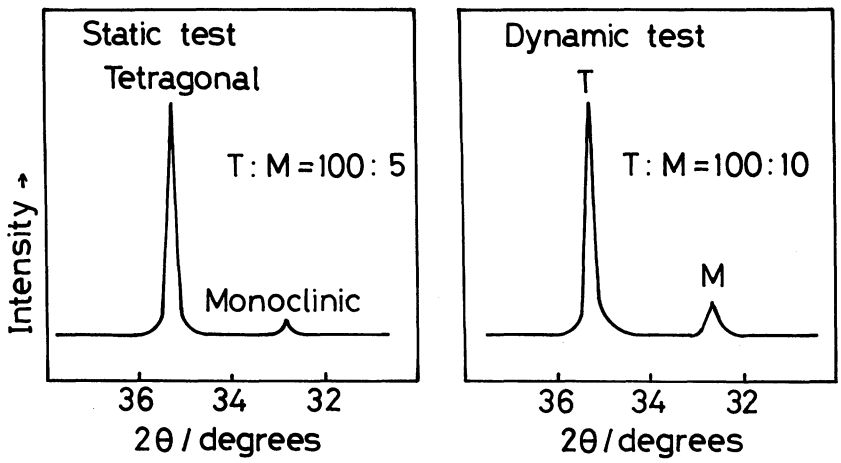

Fig. 6 X-ray diffraction patterns from fracture surface of PSZ(b).

the thermal conductivity and t is the time required to attain K_{max}. $h(\delta)$ is a nondimensional function of δ.

$$\delta=2at/w, \tag{10}$$

where a is the thermal diffusion coefficient and w is the plastic zone size. $h(\delta)$ is a monotonous decreasing function of δ and varies only near $\delta=1$. That is, when $\delta\ll1$, $h(\delta)=1$ and when $\delta\gg1$, $h(\delta)=0$.

As the plastic zone size of ceramics like PSZ is considered to be small enough to realize $\delta\gg1$ in eq. (10), the temperature rise (ΔT) at the crack tip will become zero from eq. (8).

Therefore, contrary to the metallic materials, the amount of stress-induced transformation in PSZ is larger under the dynamic loading condition, where it is said that the intersection of local shear band is apt to be easily induced[11], and therefore, some strain-induced transformation may be included. This may be a main reason of larger E_f value in the dynamic test. However, it will be necessary to investigate further details.

5. Cause of singularly oscillated loading

As mentioned before, the spiral-like loading on the load-deflection curve of the specimen PSZ(a), which has been obtained from the instrumented Charpy impact test, has been firt found in the present study. The measured period of oscillated loading τ is 2.9×10^{-5} (s).

On the other hand, the period of the normal oscillations of stress wave which is caused by inertia loading accompanying the impact is generally given by[13]

$$\tau_s=1.68(SWEBC_s)/C_0, \tag{11}$$

where C_0 is the speed of sound in the specimen, C_s is the specimen compliance, E is Young's modulus of specimen, S is the length between supports, B is the specimen thickness and W is the specimen width. τ_s of PSZ(a) specimen is calculated to be 2.1×10^{-5} (s). This value is close to the measured value of τ. Therefore, various materials have been examined by the present instrumented Charpy impact test machine to clear whether the singularly oscillated loading is observed also in other materials. Consequently, such loading has been observed only at the initial stage of load-deflection curve for the unnotched specimen of 7075 alloy. τ of this oscillated loading is 2.9×10^{-5} (s) and is in good agreement with that of PSZ(a).

The singularly oscillated loading is considered to be caused mainly by the inertial loading effect peculiar to the impact test, because the period of such loading in PSZ(a) is relatively close to the theoretically calculated one of the oscillations caused by stress wave reaction, and it has also been observed on the load-deflection curve of 7075 alloy, showing the same period with that of PSZ(a).

A load-deflection curve of PSZ(a) showing rarely incompletely oscillated loading and an X-ray diffraction pattern of the fracture surface in such a case are shown in Fig. 7①. E_t of PSZ(a) in Fig. 7① is about 70% of the same specimen which shows completely oscillated loading (Fig. 7②). Moreover, the integrated intensity ratio of monoclinic to tetragonal clearly decreases. Besides, it has been observed that this ratio also decreases in PSZ(b). This specimen size effect is somewhat mysterious; however, the stress state at the cracking site is very influential in the stress-induced transformation, and the specimen size effect may be critical. But more examinations must be made on this point.

It has been reported that the serration based on the stress-induced phase transformation appears in the static strain rate test of PSZ[14]. As mentioned before, the stress-induced phase transformation is apt to appear more easily in the dynamic test, and the singularly oscillated loading is not observed in many other materials. Therefore, such loading may be caused mainly by the stress wave generated by inertial loading at the impact and intensified by overlapping of the stress-induced phase transformation. That is, the singularly oscillated loading may be related to many microcracks formed in the transformed monoclinic phase at the crack tip (they may be formed by cracking of the secondary phase particles in the case of 7075 alloy[15]; i.e., this expansion due to microcracking at the macrocrack (pore or defect in the unnotched specimen) tip process zone is pushed back by

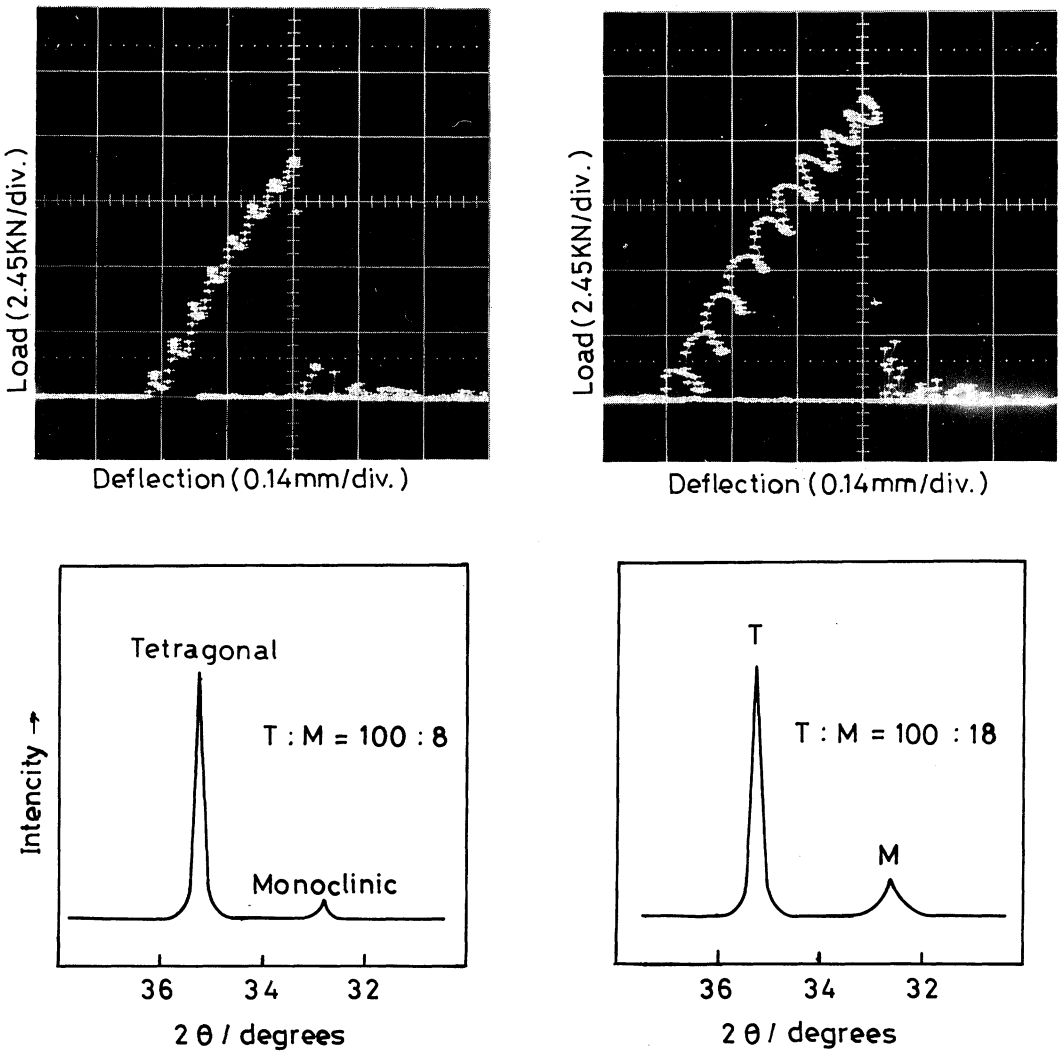

Fig. 7 Load-deflection curves and X-ray diffraction patterns of PSZ(a).

compressive inverse force from the surrounding elastic stress field. This is a so-called microcrack-induced crack closure process, see Fig. 8①. Then the macrocrack extension occurs, Fig. 8②. This is one hypothetical explanation of the singularly oscillated loading. It will be necessary, however, to investigate further details on this phenomenon in the future.

IV. Conclusion

The instrumented Charpy impact test and the static three-point bend test were carried out on PSZ and SiC to investigate the impact characteristics of ceramics. The fracture behavior of these materials was analyzed and the following results were obtained.

(1) Both of PSZ and SiC showed an elastic type brittle fracture in the instrumented impact test. The real fracture energy of PSZ was 57–59% and that of SiC was 38–56% of the total absorbed energy.

(2) The real fracture energy of PSZ in the impact test was larger than that in the static three-point bend test.

(3) The amount of stress-induced tetragonal-to-monoclinic phase transformation in the impact test was larger than that in the

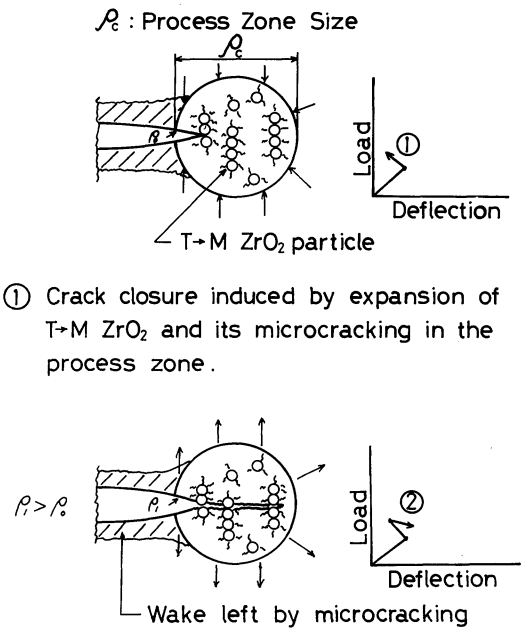

Fig. 8 Schematic explanation of singularly oscillated loading in PSZ.

static three-point bend test.

(4) Singularly oscillated loading was found on the load-deflection curve of PSZ in the impact test. This phenomenon may be due to the oscillation caused by inertial loading accompanying the impact, and it was intensified by the stress-induced phase transformation. Such hypothetical explanation was presented. However, it will be necessary to investigate further details in the future.

Acknowledgement

The authors wish to thank Sumitomo Electric Industries, Ltd. for the financial and experimental supports on this work.

REFERENCES

(1) R. C. Lueth: ASTM STP 563, (1974), p. 166.
(2) A. Dinsdale, A. J. Moulson and W. T. Wilkinson: Trans. Br. Ceram. Soc., **61** (1962), 259.
(3) T. Kobayashi: Eng. Fract. Mech., **19** (1984), 49.
(4) T. Kobayashi: J. Iron Steel Inst. Japan, **71** (1985), 654 (in Japanese).
(5) K. R. Iyer and R. B. Miclot: ASTM STP 563, (1974), p. 146.
(6) J. G. Williams: *Fracture mechanics of polymers*, Ellis Horwood Ltd., New York, (1984), p. 237.
(7) N. Claussen and M. Ruhel: *Advances in Ceramics*, Vol. 3, Am. Ceram. Soc. Inc., (1981), 137.
(8) R. C. Garvie, R. H. Hannink and R. T. Pascoe: Nature, **258** (1975), 703.
(9) S. Wakayama, T. Kishi and S. Kohara: Proc. of the Japan Inst. of Metals, (April, 1958), 224 (in Japanese).
(10) W. W. Gererich, P. L. Hemmings, V. F. Zackay and E. R. Parker: Univ. of Calif., UCRL-18467 (Sept., 1969).
(11) L. E. Murr, K. P. Standhammer and S. S. Hecker: Met. Trans., **13A** (1982), 627.
(12) J. R. Rice and N. Lavy: *Physics of Strength and Plasticity*, Ed. by A. S. Argon, The M.I.T. Press, (1969), p. 277.
(13) W. L. Server: J. Test. Eval., **6** (1978), 29.
(14) J. Lankford: J. Mater. Sic., **20** (1985), 53.
(15) T. Kobayashi: J. Jpn. Inst. Light Met., **32** (1982), 539 (in Japanese).